CSIRO PUBLISHING

Research Note

www.publish.csiro.au/journals/ijwf *International Journal of Wildland Fire*, **2007**, *16*, 341–348

Estimation of shrub height for fuel-type mapping combining airborne LiDAR and simultaneous color infrared ortho imaging

David Riaño[A,B,F], *Emilio Chuvieco*[A], *Susan L. Ustin*[B], *Javier Salas*[A], *José R. Rodríguez-Pérez*[C], *Luis M. Ribeiro*[D], *Domingos X. Viegas*[D], *José M. Moreno*[E] *and Helena Fernández*[E]

[A]Departamento de Geografía, Universidad de Alcalá, Colegios 2, E-28801 Alcalá de Henares, Madrid, Spain.

[B]Center for Spatial Technologies and Remote Sensing (CSTARS), University of California, Davis, 250-N, The Barn, One Shields Avenue, Davis, CA 95616-8617, USA.

[C]Área de Ingeniera Cartográfica, Geodésica y Fotogrametría, Universidad de León, Avenida de Astorga, s/n, E-24400 Ponferrada, León, Spain.

[D]Centro de Estudios sobre Incêndios Florestais, Coimbra, Portugal.

[E]U. Castilla la Mancha, Toledo, Spain.

[F]Corresponding author. Email: driano@cstars.ucdavis.edu

Abstract. A fuel-type map of a predominantly shrub-land area in central Portugal was generated for a fire research experimental site, by combining airborne light detection and ranging (LiDAR), and simultaneous color infrared ortho imaging. Since the vegetation canopy and the ground are too close together to be easily discerned by LiDAR pulses, standard methods of processing LiDAR data did not provide an accurate estimate of shrub height. It was demonstrated that the standard process to generate the digital ground model (DGM) sometimes contained height values for the top of the shrub canopy rather than from the ground. Improvement of the DGM was based on separating canopy from ground hits using color infrared ortho imaging to detect shrub cover, which was measured simultaneously with the LiDAR data. Potentially erroneous data in the DGM was identified using two criteria: low vegetation height and high Normalized Difference Vegetation Index (NDVI), a commonly used spectral index to identify vegetated areas. Based on the height of surrounding pixels, a second interpolation of the DGM was performed to extract those erroneously identified as ground in the standard method. The estimation of the shrub height improved significantly after this correction, and increased determination coefficients from $R^2 = 0.48$ to 0.65. However, the estimated shrub heights were still less than those observed in the field.

Additional keywords: color infrared ortho image, fuel types, LiDAR, shrub height.

Introduction

A fuel type is defined as 'an identifiable association of fuel elements of distinctive species, form, size, arrangement and continuity that will exhibit characteristic fire behavior under defined burning conditions' (Merrill and Alexander 1987). Since fuel characteristics have a strong influence in predicting fire behavior, improving fire risk estimation and fire effects assessment (e.g. gas emissions, regeneration capacity), accurate information on fuel types is critical in most phases of fire management (Chuvieco *et al*. 2003). In addition to classifying fuel types, the estimation of fuel height is commonly used as a good proxy of plant biomass and particle-size distribution. Plant height increases rapidly during the early post-fire years, and implies a rapid increase of fire hazard in a given area. Assessing fuel build-up on large scales will improve management of fire-prone areas, and advance current efforts to perform prescribed burning in those areas identified as most dangerous.

Shrub fuel types are commonly classified according to height, which corresponds to different fire behavior. For example, the European Prometheus fuel-type classification system, used by Riaño *et al*. (2002), distinguishes three different heights: surface shrubs (<0.6 m), medium-height shrubs (0.6–2 m) and tall shrubs (2–4 m). Similar approaches follow the classification of the Northern Forest Fire Laboratory (NFFL) (Albini 1976; Anderson 1982) and the National Fire Danger Rating System (NFDRS) (Deeming *et al*. 1978). Shrub height is traditionally determined in the field using transects and a measuring tape, but this technique can only inform about the spatial distribution at a very local scale. Passive remote sensing can provide vegetation percentage cover estimates from the analysis of the spectral response and spatial texture that is only indirectly related to shrub height (Riaño *et al*. 2002).

Research using airborne light detection and ranging (LiDAR) generally focuses on estimating tree parameters such as height,

10.1071/WF06003 1049-8001/07/030341

biomass, crown diameter or crown volume (Riaño *et al*. 2003; Morsdorf *et al*. 2004). Since there is a large gap in height between them, laser pulses that hit the ground are generally well discerned from ones than hit within tree canopies or branches. Therefore, tree height estimations from LiDAR are generally very accurate (Riaño *et al*. 2004).

Shrub height differentiation can be done with airborne LiDAR scanners, because they provide height accuracy up to 5–15 cm (Baltsavias 1999*a*). However, laser pulses that hit within shrub canopies are often misclassified as ground rather than canopy, which can cause severe accuracy problems when estimating shrub height. Weltz *et al*. (1994) have demonstrated the ability to measure shrub height using a pioneering airborne LiDAR profiler. Rango *et al*. (2000) have further established that shrub coppice dunes could be identified on color infrared images, and that an underestimated shrub height could be extracted from airborne LiDAR. Marsh vegetation height has also been underestimated (Rosso *et al*. 2006).

The main purpose of this study is to evaluate the efficiency of LiDAR data to obtain shrub height in order to distinguish shrub fuel types for fire management applications. If LiDAR estimations are accurate enough for shrub height mapping, this data could improve operational use of fire behavior models, which often lack accurate descriptions of fuel conditions, especially from the under story layers. In addition, LiDAR estimations provide a spatial view of observed areas, which overcomes difficulties in obtaining the same data from traditional fieldwork. Therefore, this information will greatly enhance spatial analysis of fire behavior and fire risk.

Methods

Gestosa is a fire research experimental site for shrub vegetation located in central Portugal (Fig. 1). The main shrub species of this region are *Erica australis* L., *Erica umbellata* L., *Pterospartum tridentatum* (L.) Willk and *Halimium alyssoides* (Lam.) C. Koch, which generally have a high density of more than 80%. In recent years, this area has been used extensively for experimental burnings for European fire-research projects (Viegas *et al*. 2002; Allgöwer *et al*. 2003).

Average shrub height was calculated in the field for 33 plots (Fig. 1). Twenty-nine plots were measured using one, two or three transects depending on plot size. The height of all individual plants were measured in plots 503, 504, 508 and 512, and three 2 m by 2 m subplots were averaged within each plot (Table 1). The average standard deviation (s.d.) of all plant individuals for these four plots was 0.27 m. Plots were quite homogeneous not only in height but also in spectral response. The Normalized

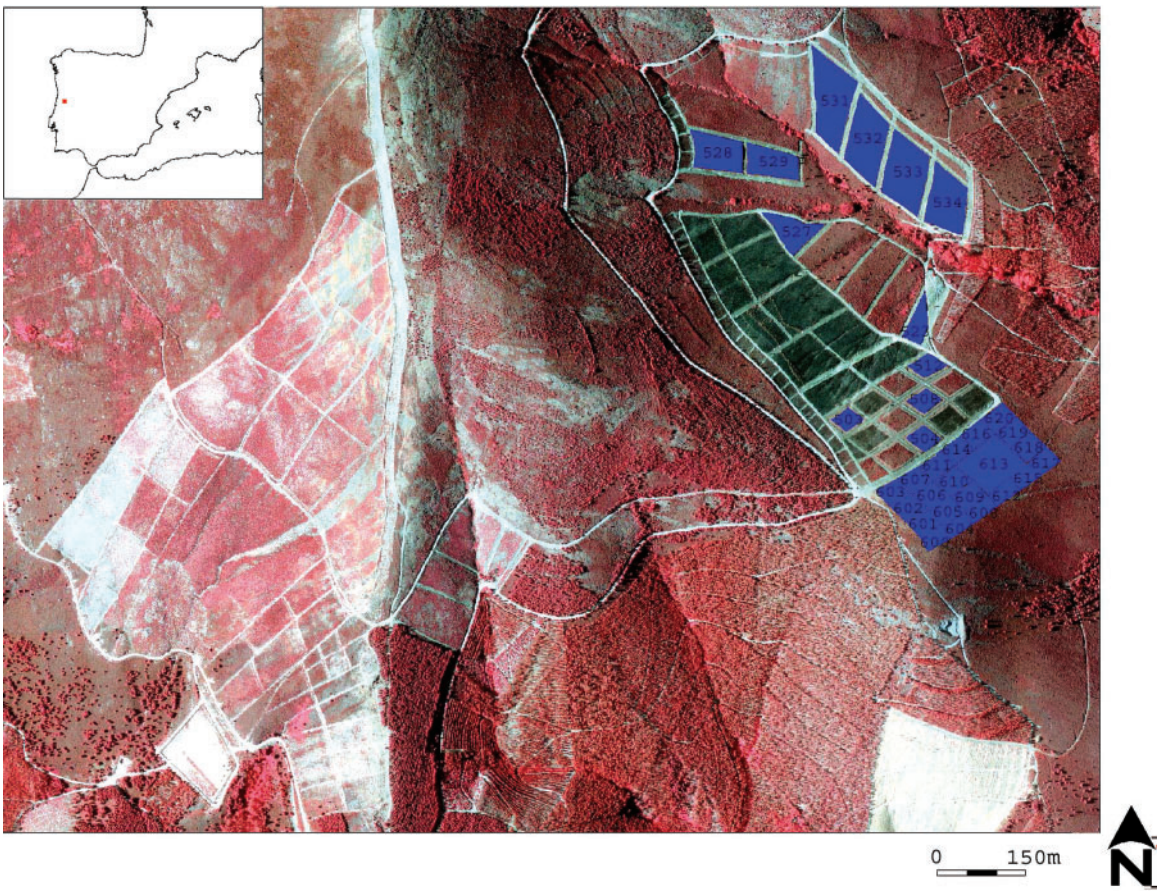

Fig. 1. Color infrared ortho image in greyscale of the study area, Gestosa (Portugal). The location of thirty-three sampled plots are shown in white with identification numbers on top.

Difference Vegetation Index (NDVI) values, a spectral index to identify vegetated areas (Carlson and Ripley 1997), increased with shrub height (Table 1), with an average s.d. of 0.18. Plot size was selected according to the different burning experiments that were to take place in the study site. Plots were easy to identify in the image, since several firebreaks were constructed around each plot before image acquisition (Fig. 1), thus ensuring the correspondence between the field measurements and the image data.

An area of 1882 m by 1422 m (longitude, 8°09′32.57′–8°10′51.95’ W; latitude, 40°02′16.89’–40°03′02.94’ N, ellipsoid: Hayford 1924, datum: European 1950) was over flown in August 2002 with the Toposys II LiDAR system (Baltsavias 1999*b*), which is also called FALCON II (http://www.toposys.com). Airborne LiDAR measures the time–distance to an intercepted point on the ground using a scanner that emits a high laser pulse frequency (Wehr and Lohr 1999). The flying height was ∼1000 m and the scan angle was ±7°, which renders a scan width of ∼250 m. This LiDAR system recorded first and last laser returns (first and last intercepted return) with a 0.5-m footprint diameter at a spatial density of 3.5 points m^{-2}, 1.95 m and 0.15 m in the across track and along the track direction, respectively. The recording height accuracy was claimed to be 0.20 m. A simultaneous color infrared ortho image, with spectral bands in the blue (450–490 nm), green (500–580 nm), red (580–660 nm) and near infrared (770–890 nm), was also acquired at 0.5-m spatial resolution (Fig. 1). The data provider, Toposys, generated a 1-m resolution digital surface model (DSM) and a digital ground model (DGM) based on the bisection principle (von Hansen and Vögtle 1999). The DSM is defined as the upper height of the ground vegetation cover, while the DGM is defined from the baseline ground surface height. The color infrared image was ortho rectified taking the LiDAR DSM as reference. The ortho images were resampled to 1 m to match the DSM and DGM.

Table 1. Average shrub height, plot size, number of field transects and average Normalized Difference Vegetation Index (NDVI) for each shrub plot

Plot	Height (m)	Size (m^2)	Transects	NDVI
523	1.11	1949	1	0.27
527	1.02	3290	2	0.36
528	1.26	4781	2	0.47
529	1.16	4054	2	0.38
531	0.64	8306	2	0.14
532	0.74	7077	2	0.22
533	1.00	7539	2	0.25
534	0.91	5997	2	0.24
503	0.85	1088	Individuals	0.32
504	0.88	1384	Individuals	0.33
508	1.68	1268	Individuals	0.45
512	1.51	1379	Individuals	0.38
600	0.89	1183	1	0.31
601	0.70	1528	1	0.24
602	0.51	1647	1	0.26
603	0.50	1443	1	0.23
604	1.08	1146	1	0.41
605	0.87	1473	1	0.36
606	0.90	1565	1	0.35
607	0.84	1470	1	0.35
608	0.93	1214	1	0.39
609	1.06	1633	1	0.40
610	1.18	1745	1	0.46
611	0.92	1507	1	0.34
612	1.34	1274	1	0.60
613	1.05	6400	3	0.46
614	1.06	1390	1	0.38
615	1.15	1116	1	0.54
616	1.03	1537	1	0.35
617	1.20	1512	1	0.48
618	1.08	1611	1	0.46
619	1.08	1551	1	0.45
620	1.10	1518	1	0.43

From these standard products, it was straightforward to estimate vegetation height as the simple difference between DSM and DGM. However, problems with these estimations were observed, since in the dense shrub canopy of the study area, on several occasions laser pulses from the canopy were identified as ground pulses, which therefore created inaccuracies in the DGM for those areas. Shrub height values were also unrealistically close to zero, since both DSM and DGM had similar values.

It was difficult to differentiate between false and true ground hits because of the low height of shrubs and the rough topography of the study area. An alternative way to improve the DGM was to identify which pulses actually came from the shrub canopy by using the spectral information derived from the color infrared ortho image acquired simultaneously with the LiDAR data. The identification of vegetation hits was based on the spectral contrast between bare soil background and vegetation cover that is clearly observed in red and near-infrared reflectance (Carlson and Ripley 1997). In the former band, the leaves present low reflectance because of the chlorophyll absorption, while in the latter, the reflectance is much higher because of the multiple scattering in the mesophyll layer. This contrast is not observed in other land cover types, such as bare soil, and therefore the higher the reflectance contrast between near-infrared and red reflectance, the more likely it is that the cover is dense and healthy in vegetation. This is the basis of most spectral vegetation indices that are routinely used for monitoring vegetation trends at local and global scales.

For this study the identification of vegetation LiDAR hits was based on using a well-known vegetation index, NDVI, defined as the difference divided by the sum of near-infrared and red channels (Carlson and Ripley 1997). The NDVI was computed from un-calibrated near-infrared and red digital values from the color infrared ortho image, which were resampled to the same resolution as the LiDAR grid. A cross-section over shrub vegetation and bare soil background is represented in Fig. 2, which shows the higher NDVI over shrub vegetation compared to the un-vegetated background.

The following classification rules were tested as a basis to identify vegetated LiDAR pulses, where height information came from the vegetation canopy (Fig. 3):

$$\text{if height } (H = \text{DSM} - \text{DGM}) < X \text{ and NDVI} > Y \text{ then}$$

$$\text{DGM} = \text{false}$$

else

$$\text{DGM} = \text{true}$$

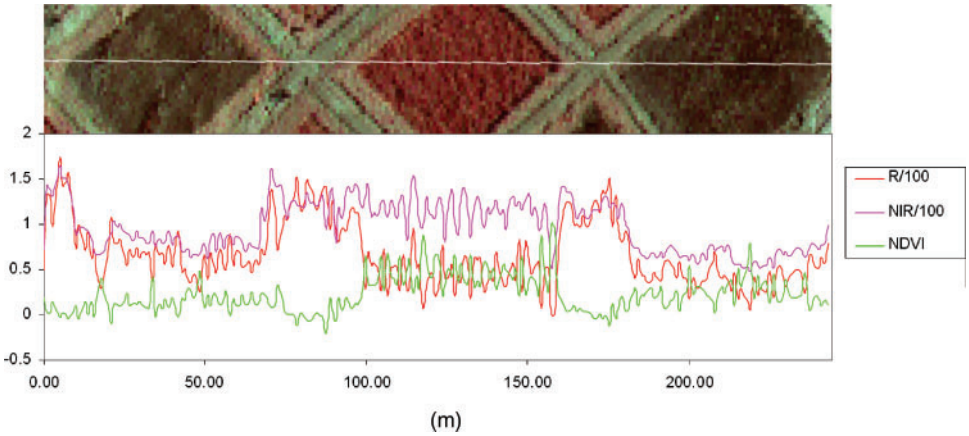

Fig. 2. Near-infrared reflectance (NIR), red reflectance (R) and Normalized Difference Vegetation Index (NDVI) cross-section over bare soil background and shrub vegetation.

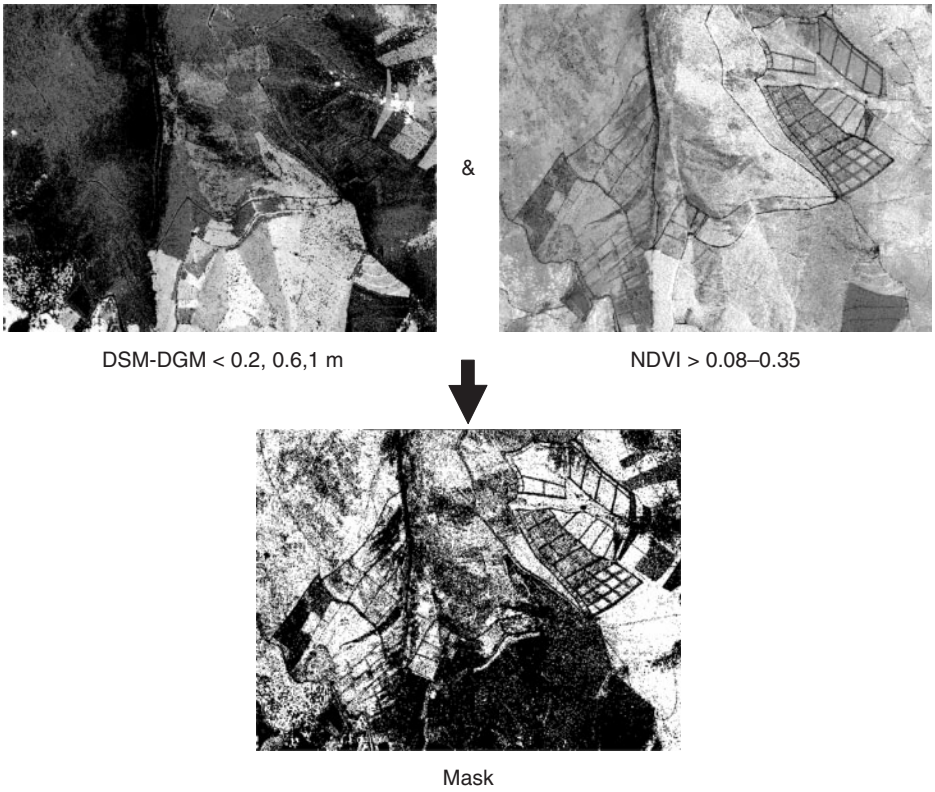

Fig. 3. Generation of mask to identify erroneous pixels in the digital ground model (DGM).

When the DGM was false, the pixel was deleted from the base elevation grid to compute a corrected DGM. Height (X) and NDVI (Y) were iteratively changed to study the improvements in final height estimation from several threshold values. The X (threshold of height difference) was changed to 0.2, 0.6 or 1 m, while Y (threshold of NDVI) was changed from 0.08 to 0.35 every 0.01. Because NDVI comes from un-calibrated near-infrared and red channels, the NDVI threshold applied in this work cannot be extrapolated to other studies. DGM height was recalculated for the erroneous (false) pixels using spatial interpolation techniques (Fig. 4). We applied a morphology dependent interpolation procedure by means of a conic search using the software PCI Geomatics 9.1 (www.pcigeomatics.com, Canada). To avoid interpolating over large areas that had no valid data in the DGM, the models were forced to select erroneous pixels in areas smaller than a window of 11 m by 11 m. Therefore, it was assured that a valid value was found at least every 5 m.

Since the field data were obtained at the plot level, the correlation between LiDAR-estimated height and field-measured height was based on extracting the average LiDAR height for

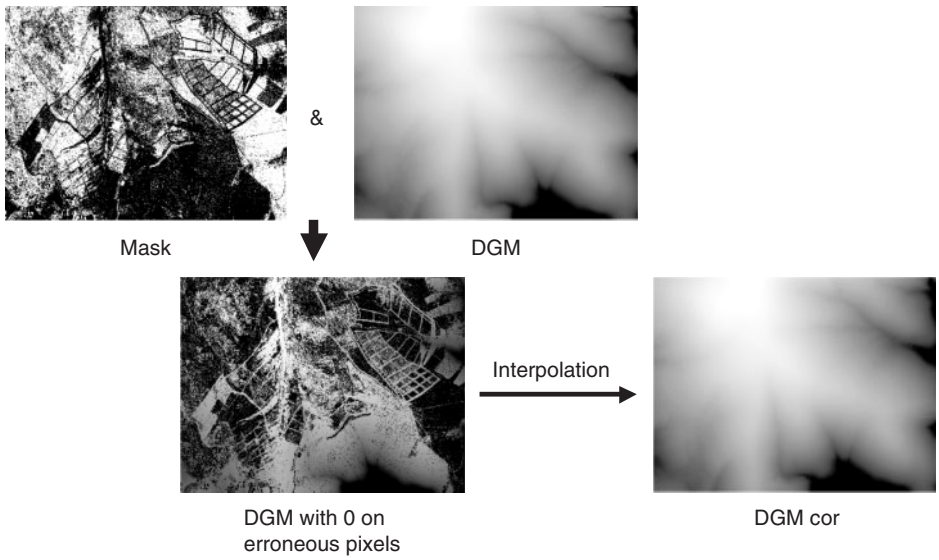

Fig. 4. Linear interpolation for the generation of the corrected digital ground model (DGM).

Table 2. Shrub height estimation (DSM−DGM) from the standard Toposys DGM generation techniques

Field-derived height and LiDAR-derived height were the dependent and independent variable, respectively. Average and standard deviation plot field derived height was 1.01 m and 0.25 m, respectively

Estimation	Slope	Intercept (m)	R^2	P-value	RMSE (m)
90th percentile	2.28	0.67	0.48	<0.001	0.18
Mean	1.31	0.76	0.20	0.009	0.22

each plot. The 90th percentile of all heights in the plot was also extracted to avoid the influence of extreme cases. Fitting between LiDAR and field data was measured from the Pearson determination coefficient (R^2) and the root mean squared error (RMSE) between observed and predicted plot shrub height values.

Results

Shrub height estimates using the DSM minus DGM generated through the standard Toposys methods is presented in Table 2. The 90th percentile provided a better result than the average value, but the slope does not follow a 1 : 1 relationship with the field data. In both cases, the R^2 values are low, which confirms the poor accuracy of the standard methods of deriving DGM in areas of low and close vegetation cover.

The generation of a new DGM based on the vegetation mask significantly improved estimates of shrub height (Fig. 5). The RMSE decreased from 0.18 m to 0.15 m, although changes in the height or NDVI thresholds for creating the vegetation mask implies fluctuations. The best results were found using a shrub height limit of <0.6 m. A higher limit implied that more pixels could be corrected. The best NDVI corrections were encountered for NDVI values >0.15 to >0.25, with most stable results for the mean value. Lowering the NDVI threshold implied a higher number of pixels to be corrected and, therefore, a decrease also in DGM values.

NDVI combined with the height limit correction caused the predictive slope to be closer to a 1 : 1 relationship. Based on the slope, R^2 and RMSE, the 90th percentile was a much better predictor of shrub height. The intercept did not vary much among corrections with values between 0.6 and 0.8 m. The best result from the vegetation masking was used to obtain a shrub fuel-type map of the study area (Fig. 6).

Discussion

The DGM created from standard techniques used to process LiDAR data in this study area clearly contained information from the vegetation canopy. The contour lines generated from the standard DGM clearly show how ground heights were erroneously identified with shrub heights (grey lines, Fig. 7). As observed in the white lines shown in Fig. 7, the corrected contour lines derived from the interpolation of the DGM after vegetation masking produced a better adaptation to the measured ground height.

The upper range of shrub height limit and NDVI values tested to build the mask was adequate, since R^2 had a maximum within the centre of the distribution and decreased in both directions. The lower shrub height limit of <0.2 m required almost no correction, since those pixels that were identified as vegetation according to NDVI had higher height values. On the other hand, a shrub height limit of <1 m removed not only vegetation but also true ground pixels, since shrubs had heights measured in the field between 0.50 and 1.68 m. The use of a lower minimum NDVI caused the slope to be much closer to a 1 : 1 relationship (Fig. 5), but R^2 was lower probably because too many pixels were included in the mask. The error distribution was significantly positively correlated with NDVI, meaning that the error was larger for plots with higher NDVI, which also had higher shrub height.

The standard height difference between the DSM and DGM provided inaccurate estimations of shrub height, which led to

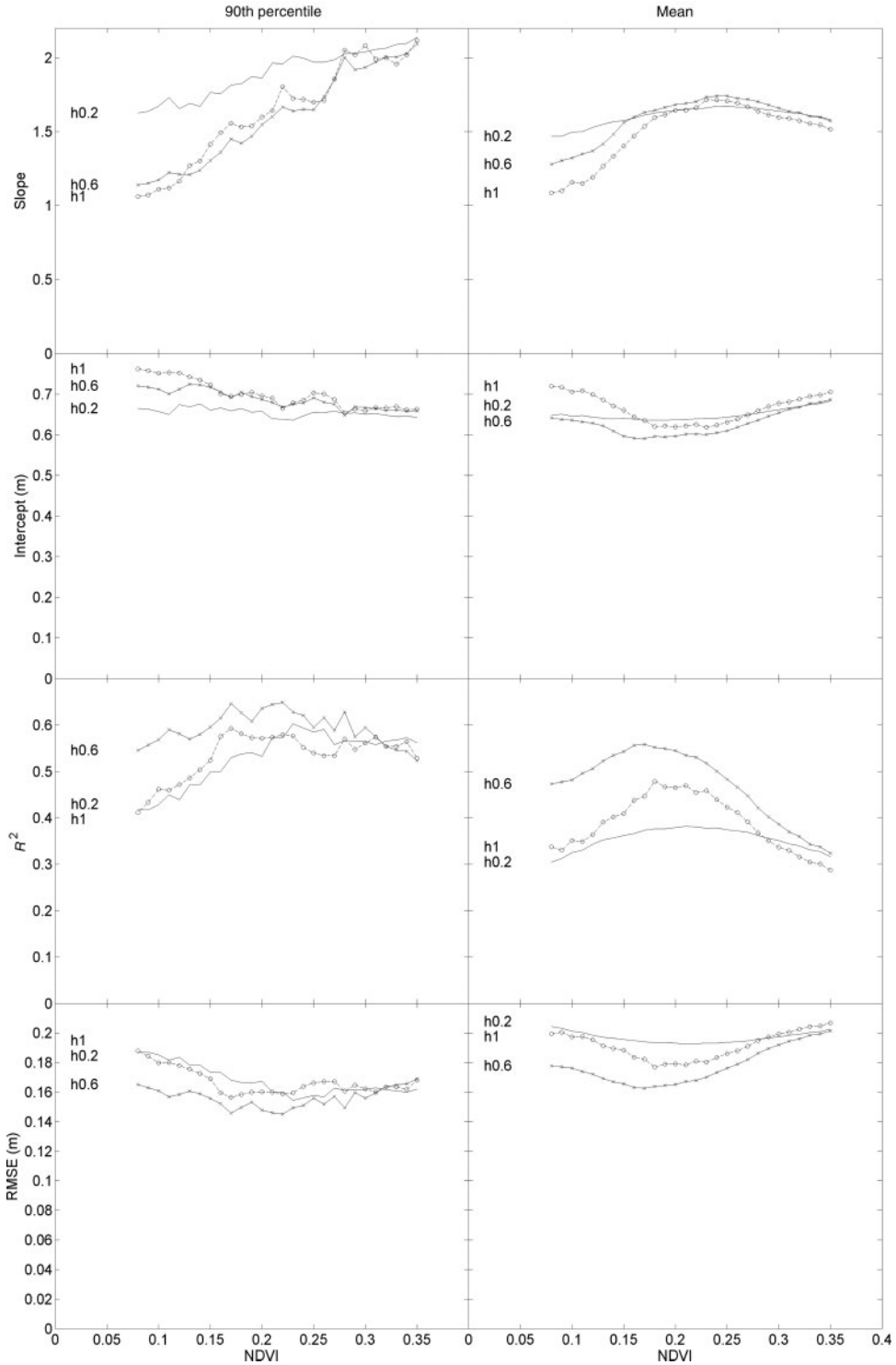

Fig. 5. Shrub height estimation using 90th percentile and mean plot value ($n = 33$). Slope, intercept, R^2 and root mean squared error (RMSE) are represented for Normalized Difference Vegetation Index (NDVI) values from >0.08 to >0.35 and vegetation heights under 0.2 (line), 0.6 (line with crosses) and 1 m (line with circles). P-value <0.001 in all cases. Field-derived height and LiDAR-derived height were the dependent and independent variable, respectively. Average and standard deviation plot field-derived height was 1.01 m and 0.25 m, respectively.

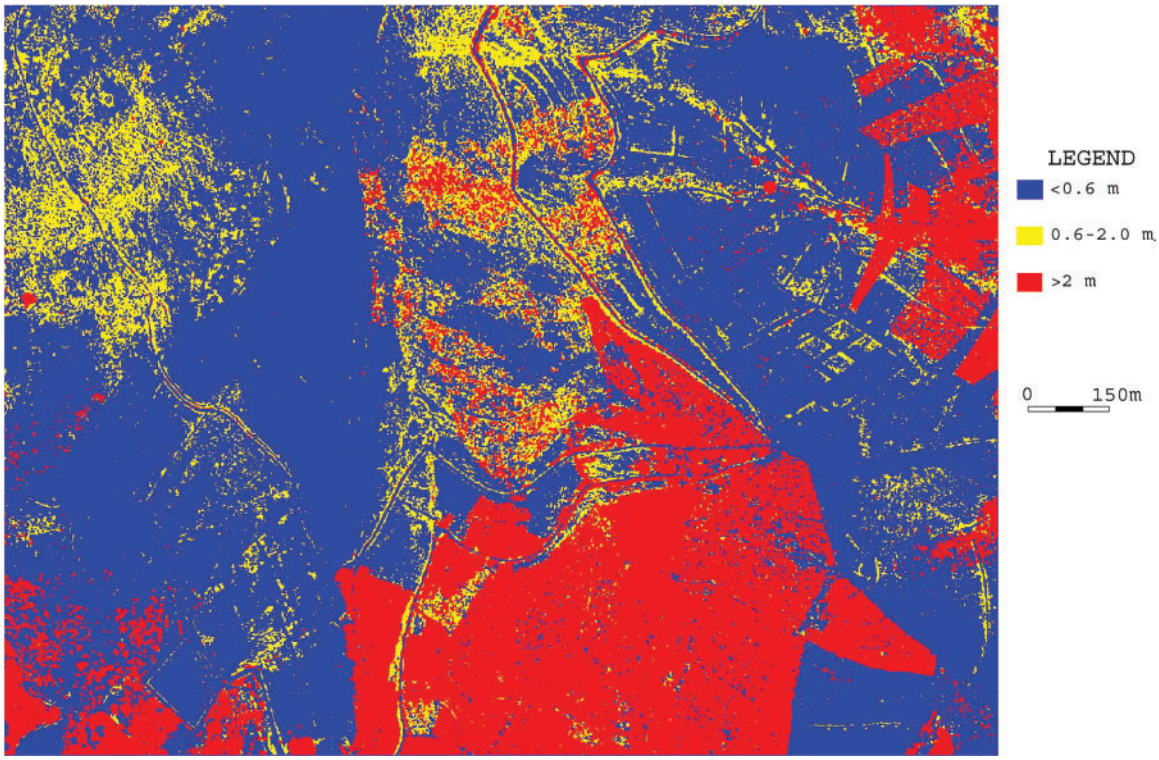

Fig. 6. Shrub fuel-type map generated by combining LiDAR with color infrared ortho image using Normalized Difference Vegetation Index (NDVI) >0.11 and height <0.6 m.

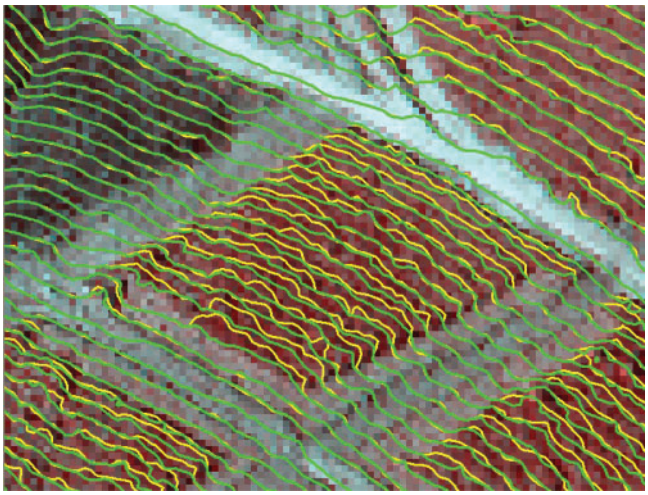

Fig. 7. Color infrared ortho image with uncorrected (grey) and corrected (white, Normalized Difference Vegetation Index (NDVI) >0.11 and height <0.6 m) contour lines from the digital ground model (DGM).

poor correlations between LiDAR estimates and field measurements. The DGM was generated based on a slope threshold between neighboring LiDAR hits. If the slope between an initial ground LiDAR hit and its neighbor was large enough it was identified as belonging to the vegetation canopy. The small difference in height, between shrub height and ground, made it harder to determine the proper slope thresholds to distinguish vegetation from ground hits. Given that some laser returns, used to build the DSM, were not coming from the top, but somewhere in between the ground and the top of the canopy, the 90th percentile predicted better shrub height than the plot average. The mean was more sensitive to those laser returns than at the 90th percentile.

Validation of the DSM and DGM was performed in 33 plots, which had small height ranges. This range is at the limit of recording accuracy for the LiDAR instrument. Since the intercept did not change, an under-estimation of the shrub height was still encountered after the correction of 0.6–0.8 m. This effect was also observed in a previous study on shrub coppice dunes (Rango *et al*. 2000). Gaveau and Hill (2003) quantified a 1.02-m underestimation in tall shrubs of 4 to 8 m. Therefore, it is difficult to discern shrub fuel types of less than 0.6-m height with LiDAR data since it could be confused with ground observations, unless color infrared ortho imaging analysis is included to differentiate between vegetation canopy and bare ground. The combination of airborne LiDAR with color infrared ortho imaging served to identify pixels in the DGM that were derived from the vegetation. Once these pixels were removed, the overall shrub height estimation was clearly improved.

The final vegetation and terrain maps can be used to improve accuracy in fire behavior modeling or to estimate fire biomass consumption. We could also relate LiDAR shrub height to shrub biomass. Riaño *et al*. (2004) related tree foliar biomass to mean LiDAR height and 99th percentile. Additional tests for a set of classification rules are to be used to identify mixed information coming from the ground or the vegetation in the DGM. The method that maintains the slope close to a 1 : 1 relationship with a high R^2 and low RMSE should be selected. In our case (Fig. 5),

an appropriate solution for this identification was NDVI >0.11 and vegetation height <0.6 m.

The shrub fuel-type map (Fig. 6) provides a spatial representation of shrub height variation, which can be directly linked to spatial models of fire behavior (Finney 1998), or fire effects assessment (Reinhardt *et al*. 2001).

Acknowledgements

This work was funded by the EC project 'Forest Fire Spread and Mitigation (SPREAD)', EC-Contract Nr. EVG1-CT-2001-00027. The Ministry of Science and Technology 'Ramón y Cajal' Program supported David Riaño. Thanks to Keir Keightley and Marco Trombetti for reviewing this manuscript. Linguistic assistance from Julia Marcia Medina is also acknowledged.

References

Albini FA (1976) 'Estimating wildfire behavior and effects.' USDA, Forest Service, Intermountain Forest and Range Experiment Station, INT-30. (Ogden, UT)

Allgöwer B, Benvenuti M, Bowyer P, Camia A, Chuvieco E, Danson M, Giakoumakis M, Gitas I, Morsdorf F, Riaño D, Viegas DX, Vanhamajamaa I (2003) 'Methods to map fuel types from remotely sensed data.' Deliverable 111. SPREAD PROJECT. EVG1-CT-2001–00043.

Anderson HE (1982) 'Aids to determining fuel models for estimating fire behavior.' USDA, Forest Service, General Technical Report INT-122. (Ogden, UT)

Baltsavias EP (1999*a*) Airborne laser scanning: basic relations and formulas. *ISPRS Journal of Photogrammetry and Remote Sensing* **54**, 199–214.

Baltsavias EP (1999*b*) Airborne laser scanning: existing systems and firms and other sources. *ISPRS Journal of Photogrammetry and Remote Sensing* **54**, 164–198.

Carlson TN, Ripley DA (1997) On the relation between NDVI, fractional vegetation cover, and leaf area index. *Remote Sensing of Environment* **62**, 241–252.

Chuvieco E, Riaño D, Van Wagtendonk JW, Morsdorf F (2003) Fuel loads and fuel types. In 'Wildland Fire Danger Estimation And Mapping. The Role of Remote Sensing Data'. (Ed. E Chuvieco) pp. 1–32. (World Scientific Publishing Co. Ltd.)

Deeming JE, Burgan RE, Cohen JD (1978) 'The National Fire-Danger Rating System – 1978.' USDA Forest Service, GTR INT-39. (Ogden, UT)

Finney MA (1998) 'FARSITE: Fire Area Simulator – Model development and evaluation.' USDA Forest Service, Rocky Mountain Research Station, RMRS-RP-4. (Ogden, UT)

Gaveau DLA, Hill RA (2003) Quantifying canopy height underestimation by laser pulse penetration in small-footprint airborne laser scanning data. *Canadian Journal of Remote Sensing* **29**, 650–657.

Merrill DF, Alexander ME (1987) 'Glossary of forest fire management terms.' National Research Council of Canada, Committee for Forest Fire Management. (Ottawa, ON)

Morsdorf F, Meier E, Kotz B, Itten KI, Dobbertin M, Allgower B (2004) LIDAR-based geometric reconstruction of boreal type forest stands at single tree level for forest and wildland fire management. *Remote Sensing of Environment* **92**, 353–362.

Rango A, Chopping M, Ritchie J, Havstad K, Kustas W, Schmugge T (2000) Morphological characteristics of shrub coppice dunes in desert grasslands of southern New Mexico derived from scanning LIDAR. *Remote Sensing of Environment* **74**, 26–44.

Reinhardt ED, Keane RE, Brown JK (2001) Modeling fire effects. *International Journal of Wildland Fire* **10**, 373–380.

Riaño D, Chuvieco E, Condés S, González-Matesanz J, Ustin SL (2004) Generation of crown bulk density for *Pinus sylvestris* L. from lidar. *Remote Sensing of Environment* **92**, 345–352.

Riaño D, Chuvieco E, Salas J, Palacios-Orueta A, Bastarrika A (2002) Generation of fuel type maps from Landsat TM images and ancillary data in Mediterranean ecosystems. *Canadian Journal of Forest Research-Revue Canadienne de Recherche Forestier* **32**, 1301–1315.

Riaño D, Meier E, Allgöwer B, Chuvieco E, Ustin SL (2003) Modeling airborne laser scanning data for the spatial generation of critical forest parameters in fire behavior modeling. *Remote Sensing of Environment* **86**, 177–186.

Rosso PH, Ustin SL, Hastings A (2006) Use of lidar to study changes associated with Spartina invasion in San Francisco Bay marshes. *Remote Sensing of Environment* **100**, 295–306.

Viegas DX, Cruz MG, Ribeiro LM, Silva AJ, Ollero A, Arrue B, Dios R, Gómez-Rodríguez F, Merino L, Miranda AI, Santos P (2002) Gestosa fire spread experiments. In 'Forest Fire Research & Wildland Fire Safety'. (Ed. DX Viegas) (Millpress: Rotterdam, Netherlands)

von Hansen W, Vögtle T (1999) Extraktion der Geländeoberfläche aus flugzeuggetragenen Laserscanner-Aufnahmen. *Photogrammetrie Fernerkundung Geoinformation* **4**, 229–236.

Wehr A, Lohr U (1999) Airborne laser scanning – an introduction and overview. *ISPRS Journal of Photogrammetry & Remote Sensing* **54**, 68–82.

Weltz MA, Ritchie JC, Fox HD (1994) Comparison of Laser and Field-Measurements of Vegetation Height and Canopy Cover. *Water Resources Research* **30**, 1311–1319.

Manuscript received 6 January 2006, accepted 24 January 2007